THE JOURNAL OF PHYSICAL CHEMISTRY B

Article

pubs.acs.org/JPCB

Patupilone and Ixabepilone: The Effect of a Point Structural Change on the Exo–Endo Conformational Profile

Marek Lozynski*

Institute of Chemical Technology and Engineering, Poznan University of Technology, Pl. M. Sklodowskiej-Curie 5, 60-965 Poznan, Poland

Supporting Information

ABSTRACT: The natural product patupilone (epothilone B) and its synthetic aza-analogue, ixabepilone, are effective agents against a broad range of human cancers. A detailed conformational analysis was conducted on the basis of single-point MP2 energy calculations for density functional theory (DFT) geometries at the MP2/6-31+G(d,p)//B3LYP/6-31+G(d,p) level. In a vacuum, patupilone exclusively adopts compact exo conformations due to short, near-linear hydrogen bonding between the 3-hydroxyl group and the side-chain thiazole. In contrast, ixabepilone can be described as a competitive mixture of exo and endo conformers with a large population of the above-mentioned compact exo conformations. The stability of the endo form is consistent with the cooperativity of hydrogen bonds. The relative energies of some patupilone and ixabepilone conformers were found to be sensitive to solvent effects within the integral equation formalism polarizable continuum model (IEF-PCM). This study contributes to a better understanding of the important structural features of patupilone and ixabepilone. This conformational analysis lends support to previous observations concerning their different pharmaceutical profiles.

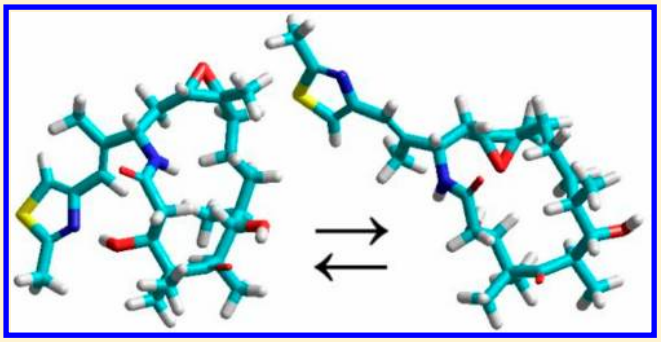

INTRODUCTION

The epothilones[1,2] were isolated from the myxobacterium *Sorangium cellulosum*.[3] Similar to the taxanes, the epothilones are cytotoxic drugs that promote the polymerization of $\alpha\beta$-tubulin heterodimers to microtubules.[4,5] Epothilones A and B (patupilone) (Scheme 1) were found to be active in vitro, but their in vivo activities are suppressed due to their limited metabolic stabilities and unfavorable pharmacokinetics.[1,6,7] Ixabepilone[6] (Ixempra, BMS-247550) (Scheme 1), a semisynthetic[8] aza-analogue of epothilone B, is the first and only representative of the epothilone family that has been approved (in October 2007) to date by the U.S. Food and Drug Administration. Ixabepilone, which has a manageable pharmacokinetic and safety profile, can be used as a first-line therapy[6,9,10] or in the adjuvant setting because it has a synergic antitumor effect when used with other chemotherapeutics agents, especially capecitabine.[11,12] Ixabepilone has a low susceptibility to common mechanisms of drug resistance, demonstrates very high efficacy against anthracycline- and taxane-resistant tumors, and is now being intensively tested for therapeutic features to define its specific area of applicability as a taxane alternative.[13]

Paclitaxel (Taxol), first used in cancer therapy as an effective microtubule-stabilizing agent (MSA), binds specifically and stoichiometrically to β-tubulin subunits.[14] The structure of paclitaxel bound to the tubulin dimer was obtained by electron crystallography of zinc-induced sheets of tubulin.[15−17] Epothilones occupy an overlapping space in the paclitaxel-binding site on microtubules,[1,18] and common pharmacophore has been proposed for these two structurally diverse chemotherapeutic agents.[19−25] However, the assumption that the relatively polar functional groups and the similar hydrophobic fragments of these ligands use the same complementary subsites of the tubulin pocket is not valid: each molecule interacts with the protein in a unique manner.[26−28] The binding of the epothilones to tubulin was also investigated by both solution-state NMR[25,29,30] and, more recently, solid-state NMR[31,32] spectroscopy. Changes in the chemical shifts upon microtubule binding suggest that the structures derived from the EC and NMR models are different as well as their molecular orientations.[25]

Recently, Horwitz et al.[33] reported a unique method for gaining insight into the mechanism of cytoskeleton stabilization by MSAs. The structural changes that occur in tubulin upon the binding of an MSA can be mapped by examining the altered levels of hydrogen/deuterium exchange (HDX) from the incorporation of deuterium into peptide bonds.[34] The markedly reduced degree of HDX upon MSA incorporation is due to decreased solvent accessibility and/or the adoption of a more rigid conformation by the α- and β-tubulin chains. In such

Received: December 31, 2011
Revised: June 5, 2012
Published: June 5, 2012

Scheme 1. Chemical Structures of Epothilone A, Patupilone, and Ixabepilone

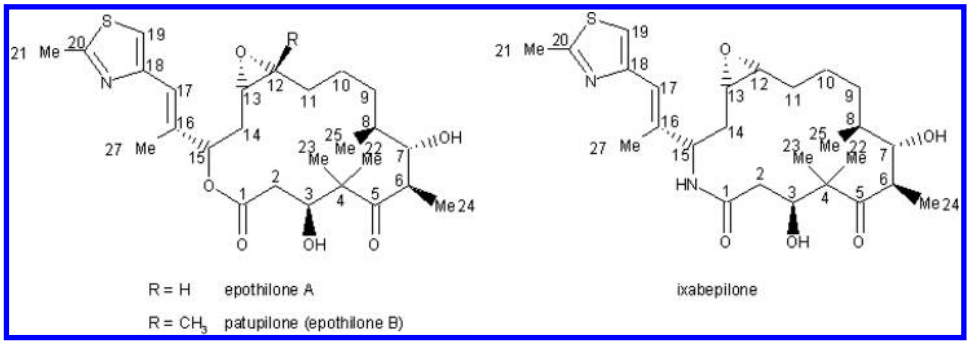

studies, the part of the drug-binding site at the N-terminal portion of the M-loop, represented by peptide β266−280, was found to be well protected from deuterium incorporation by epothilone B but not by ixabepilone.[35] Moreover, the distal part of the tubulin M-loop was greatly protected by epothilone, suggesting a considerable difference in the binding modes of these two structurally related drugs. Although both epothilone B and ixabepilone bind mainly to the taxane pocket of β-tubulin, the significant reduction in deuterium incorporation on the tubulin dimer interface when complexed with epothilone B suggests an additional area of specific interactions, and there appears to be no difference between the effects of these two drugs on the intradimer interface. Computational docking simulations based on the HDX profiles suggest a preference for binding to the taxane pocket in β-tubulin over the α-tubulin subunit. Interestingly, the two ligands exhibit different flexibilities within the binding pocket: epothilone B has one well-defined orientation at the taxane binding site, whereas ixabepilone possesses three distinct binding poses, effectively exploiting the promiscuous character of the β-tubulin binding pocket.[35]

Patupilone and ixabepilone have undergone parallel clinical development processes.[36] Although their general mechanisms of action are identical and their molecular structures are very similar, the epothilones exhibit different activities, tolerability profiles, and clinically relevant side effects.[37] In the current search for novel MSAs, three of the main objectives are to enhance tumor specificity, reduce neurotoxicity, and overcome drug resistance.[36,38] Therefore, there is an urgent need to understand not only the molecular mechanism of microtubule stabilization by existing MSAs but also the mechanism by which tumor cells became refractory to chemotherapy. Detailed knowledge of the effects of structural features on the overall molecular shape of the epothilone ligands may be helpful in the elucidation of molecular mechanisms and, perhaps, future drug design. Thus, conformational studies are required to determine the potential energy space (PES) of both epothilone B and ixabepilone. In this way, their behavior as microtubule-targeting ligands capable of triggering the in vitro growth of the cytoskeleton can be defined at the conformational level.

To date, there have been few density functional theory (DFT)-based calculations on the epothilone system. Rusinska-Roszak et al.[39] reported a computational study of an open-ring epothilone analogue. In 2009, Rusinska-Roszak et al.[40] applied DFT to analyze the interconversion between endo- and exoforms in a truncated model of epothilone A. More recently, Jimenez[41] used the B3LYP and X3LYP methods to study the PES of epothilone A and to present a minireceptor model of tubulin. Very recently, electron correlations have also been included in the calculations, and the MP2//DFT approach has been demonstrated to be an effective way to overcome the relative flatness of the DFT energy data for epothilone A.[42] The final results have been shown to be in agreement with solution NMR spectroscopy and suggest a solvent-dependent equilibrium between extended and compact (clustered[42]) forms of epothilone.

Because experimental data referring to ixabepilone are scarce and data on the conformational energy surface of epothilone B are still incomplete, I extended my studies on epothilone A to this compound following the same strategy.[42] My aim is to supply an overview of the possible unbound conformers of ixabepilone and compare them with those of patupilone, which is reported as a reference. The solvent dependence of the PES is also briefly discussed.

COMPUTATIONAL METHODOLOGY

The structural analysis of epothilone system allows one to distinguish two interconverting subsets of conformers: exo,[2] in which the epoxide bridge is arranged outward, and endo,[18] with its oxygen atom pointed inward to the macrocyclic ring. Starting molecular coordinates of the representative exo and endo forms were chosen from geometries available experimentally from X-ray crystallography (**H**,[2] **P**[43]), electron crystallography (**S**[18]), NMR spectroscopy (**M**,[29] **T**[44]), on the basis of QSAR studies (**W**[45]), and supplemented with low-energy structures **X**(exo) and **Y**(endo) from systematic, conformational search of epothilone A at the PM3 level.[41] Coordinates of epothilone A bound to tubulin **S** (1TVK) or cytochrome P450epoK **P** (1Q5D) were extracted from Protein Data Bank (PDB) files.[46]

In order to get better estimates of the molecular energies, calculations were performed with the MP2//B3LYP method.[47,48] I employed *in vacuo* MP2/6-31+G(d,p)//B3LYP6-31+G(d,p) level, which is a good compromise between the size of the system studied and the computational demand. I observed that the model chemistry used predicts the relative interaction energies spread over a much larger range than those calculated using the standard B3LYP6-31+G(d,p)// B3LYP6-31+G(d,p) optimization model.[42] The selected geometries were transformed into the patupilone and ixabepilone starting structures, as appropriate, and all of these molecules were optimized using B3LYP/6-31+G(d,p) calculations with Gaussian 09.[49] The loose convergence criteria of Gaussian program were applied (requiring the root-mean-square (rms) forces to be smaller than 1.667×10^{-3} hartree·bohr^{-1}). Frequency calculations at the B3LYP/6-31G(d) level gave no imaginary frequencies, confirming that the optimized structures are true minima. To estimate the geometry and energy changes in

dx.doi.org/10.1021/jp212628v | J. Phys. Chem. B 2012, 116, 7605−7617

Table 1. Selected Torsion Angle Values[a], Hydrogen Bond Parameters[b], and Correlated Energy Correction (MP2) Relative Energies[c] for Stable DFT Conformations of Patupilone (Epothilone B) at the MP2/6-31+G(d,p)//B3LYP/6-31+G(d,p) Level of Theory

	torsional angles					hydrogen bond distances and angles[d,e]		
	epoxide 10−11−12−O12	side chain 14−15−16−17	side chain 16−17−18−19	3-hydroxyl 2−3−O3−H3	7-hydroxyl 6−7−O7−H7	3-hydroxyl	7-hydroxyl	MP2 energies[f]
b**H01**	−169.2	−128.8	176.0	−85.3	−169.3	1.906 Å(140.5°)C	noHB	5.18
b**H02**	−176.1	−124.2	177.7	67.1	−167.1	2.172 Å(127.7°)EC	noHB	7.75
b**H03**	−176.2	−121.1	−18.5	66.7	−82.7	2.175 Å(127.7°)EC	noHB	8.01
b**H04**	−178.5	−125.9	175.6	164.8	−171.0	noHB	noHB	8.05
b**H05**	−178.3	−126.2	175.9	165.7	77.0	noHB	noHB	8.29
b**H06**	−174.7	100.7	−15.6	67.1	−82.3	2.190 Å(127.3°)EC	noHB	8.38
b**H07**	−175.0	93.9	178.9	67.5	−82.8	2.199 Å(126.9°)EC	noHB	8.52
b**H08**	−178.7	87.8	179.2	166.1	−170.1	noHB	noHB	8.57
b**H09**	−178.1	87.6	178.8	162.2	−84.1	noHB	noHB	8.79
b**H10**	−178.4	92.1	−20.8	168.7	75.5	noHB	noHB	8.80
b**H11**	−177.9	92.1	−20.8	164.2	−83.5	noHB	noHB	8.80
b**H12**	−178.5	88.1	179.4	166.8	76.8	noHB	noHB	8.93
b**H13**	−177.8	−120.3	−16.8	160.2	−84.1	noHB	noHB	8.99
b**H14**	−178.8	98.6	12.2	167.2	75.4	noHB	noHB	9.06
b**H15**	−178.2	−120.6	−17.2	164.3	76.9	noHB	noHB	9.10
b**M01**	−167.0	87.1	42.1	138.6	−166.5	2.074 Å(161.7°)thia	noHB	2.86
b**M02**	−167.6	−141.6	−141.9	121.2	−165.4	2.212 Å(151.8°)thia	noHB	3.75
b**M03**	−168.7	−117.6	−15.5	40.8	−86.2	2.037 Å(140.8°)EC	noHB	7.03
b**M04**	−169.0	−117.2	−14.8	41.0	−166.0	2.046 Å(140.5°) EC	noHB	7.27
b**M05**	−154.9	−114.5	14.8	56.0	−164.2	2.091 Å(132.1°) EE	noHB	7.35
b**M06**	−169.3	−118.2	−16.9	40.3	73.1	2.040 Å(140.7°) EC	noHB	7.95
b**M07**	−171.8	−129.6	176.6	62.6	−164.1	2.124 Å(128.6°) EE	noHB	7.97
b**M08**	−171.2	−116.1	18.5	−49.6	−164.6	*3.153 Å(96.6°) EE*	noHB	7.97
b**M09**	−169.9	94.6	−171.6	−48.4	−166.9	noHB	noHB	8.12
b**M10**	−169.6	−116.2	18.4	−49.0	−85.6	*3.147 Å(97.2°) EC*	noHB	8.27
b**M11**	−160.9	108.6	−178.3	60.6	−164.5	2.086 Å(130.5°)EE	noHB	8.27
b**M12**	−168.7	−116.1	19.0	−50.2	72.7	*3.177 Å(95.8°) EC*	noHB	8.50
b**M13**	−151.7	−5.7	−22.4	52.4	−165.9	2.115 Å(133.2°)EE	noHB	8.61
b**M14**	−151.0	−6.8	177.8	51.5	−166.0	2.113 Å(133.5°) EE	noHB	8.70
b**M15**	−162.9	107.2	−25.0	59.5	−164.2	2.110 Å(130.0°) EE	noHB	8.71
b**M16**	−175.1	25.2	179.6	65.2	−165.9	2.091 Å(127.7°) EE	noHB	9.31
b**M17**	−173.9	16.5	−18.1	68.0	−165.7	2.100 Å(126.8°) EE	noHB	9.42
b**M18**	−169.8	−121.4	−18.0	153.3	−164.9	noHB	noHB	9.48
b**M19**	−173.6	20.5	16.3	69.4	−164.5	2.127 Å(125.4°) EE	noHB	9.69
b**M20**	−167.9	−121.2	−18.2	155.5	73.0	noHB	noHB	9.98
b**N01**	32.4	−14.0	−22.5	−68.7	−57.5	2.292 Å(128.3°)C	2.148 Å(131.1°)C	9.77
b**N02**	30.3	115.8	−176.1	47.2	−53.9	noHB	2.041 Å(134.6°)C	12.06
b**N03**	30.8	113.2	19.8	53.8	−53.6	noHB	2.034 Å(134.9°)C	12.17
b**N04**	25.8	−17.2	176.6	−74.3	−55.2	2.109 Å(132.7°)C	2.015 Å(134.3°)C	12.21
b**P01**	172.6	90.5	41.7	128.8	−45.0	2.039 Å(168.5°) thia	1.973 Å(138.8°)C	0.00
b**P02**	−169.0	−140.8	−136.0	105.5	−45.3	2.105 Å(160.2°) thia	1.970 Å(138.7°)C	0.22

dx.doi.org/10.1021/jp212628v | J. Phys. Chem. B 2012, 116, 7605−7617

Table 1. continued

	torsional angles					hydrogen bond distances and angles[d,e]		
	epoxide 10−11−12−O12	side chain 14−15−16−17	side chain 16−17−18−19	3-hydroxyl 2−3−O3−H3	7-hydroxyl 6−7−O7−H7	3-hydroxyl	7-hydroxyl	MP2 energies[f]
b**P03**	−144.6	−120.3	175.2	31.4	−46.3	2.136 Å(141.7°)EC	1.999 Å(137.4°)C	4.25
b**P04**	115.4	77.5	−22.8	35.8	−47.9	2.101 Å(141.2°) EC	1.973 Å(137.7°)C	5.17
b**P05**	114.2	−120.9	174.7	30.4	−47.5	2.169 Å(141.3°) EC	1.969 Å(137.8°)C	5.42
b**P06**	115.0	−126.5	179.0	73.0	−45.5	2.504 Å(117.1°) EE	2.021 Å(137.6°)C	5.47
b**P07**	114.7	118.0	−169.1	−44.1	−47.9	*3.150 Å(98.6°) EC*	2.014 Å(137.0°)C	6.35
b**P08**	−172.8	−115.0	18.1	−45.5	−45.3	noHB	1.996 Å(138.2°)C	6.52
b**P09**	−143.2	14.6	175.6	156.2	−45.3	noHB	2.038 Å(137.0°)C	7.00
b**P10**	114.2	6.0	−24.4	−51.0	−47.5	noHB	2.002 Å(137.2°)C	8.00
b**P11**	113.2	10.9	176.2	153.3	−47.4	noHB	2.006 Å(137.1°)C	8.44
b**P12**	113.4	5.9	176.9	−50.9	−47.6	noHB	1.997 Å(137.3°)C	8.54
b**S01**	25.9	79.0	178.3	−80.5	−58.8	1.944 Å(137.8°)C	2.027 Å(132.1°)C	6.84
b**S02**	25.5	77.2	27.0	−81.1	−58.4	1.939 Å(138.2°)C	2.027 Å(132.4°)C	7.50
b**S03**	24.6	−93.9	18.3	−80.9	−58.9	1.938 Å(138.0°)C	2.023 Å(132.2°)C	8.68
b**S04**	23.3	−91.9	176.7	−80.3	−58.5	1.943 Å(137.8°)C	2.012 Å(132.7°)C	9.19
b**T01**	−171.0	81.3	−21.3	38.5	−48.7	2.133 Å(139.7°)EC	1.983 Å(137.1°)C	3.77
b**T02**	115.7	77.9	−23.0	35.3	−47.7	2.102 Å(141.2°)EC	1.968 Å(137.9°)C	5.23
b**T03**	114.7	73.7	179.1	35.4	−48.1	2.102 Å(141.0°)EC	1.975 Å(137.6°)C	5.24
b**T04**	113.6	−114.8	−11.5	30.3	−48.2	2.114 Å(142.0°)EC	1.975 Å(137.5°)C	6.47
b**W01**	−0.4	111.8	−176.9	94.1	−166.5	2.073 Å(145.9°) epo *2.660 Å(96.9°)EE*	noHB	3.57
b**W02**	1.0	105.1	−15.5	92.2	−166.1	2.111 Å(143.8°) epo *2.659 Å(98.7°)EE*	noHB	4.92
b**W03**	1.6	−109.2	173.9	92.3	−166.9	2.064 Å(145.8°) epo *2.701 Å(98.4°)EE*	noHB	4.97
b**W04**	0.4	−102.2	−12.6	94.9	−166.8	2.037 Å(147.6°) epo *2.732 Å(95.7°)EE*	noHB	5.23
b**W05**	7.3	−107.5	176.3	57.6	−167.0	noHB 2.063 Å(133.0°)EE	noHB	5.91
b**X01**	−144.0	−141.6	−131.8	103.6	−46.3	2.103(161.1°)thia	2.019 Å(137.3°)C	0.28
b**X02**	−142.8	165.0	−35.2	136.8	−45.3	2.096 Å(160.5°)thia	2.019 Å(137.5°)C	3.01
b**X03**	−144.6	−114.9	−13.2	30.6	−45.8	2.105 Å(142.1°)EC	1.996 Å(137.5°)C	4.92
b**X04**	−169.2	−127.6	174.9	−85.5	−169.7	1.908 Å(140.5°)C	noHB	5.14
b**X05**	−169.8	66.1	23.9	−84.9	−54.1	1.985 Å(138.7°)C	2.062 Å(133.3°)C	5.51
b**X06**	114.2	−122.6	−20.2	70.3	−45.7	*2.482 Å(118.4°)EE*	2.026 Å(137.4°)C	5.64
b**X07**	−154.3	−122.3	175.8	−107.7	−174.1	1.788 Å(147.3°)C	noHB	6.85
b**X08**	−156.5	−121.6	−16.6	−77.0	−53.5	*2.371 Å(117.0°)EC* 2.196 Å(124.5°)C	1.985 Å(136.0°)C	7.34
b**X09**	−149.0	−120.8	−18.9	165.5	−47.3	noHB	2.067 Å(136.3°)C	7.37
b**X10**	48.8	−120.1	−17.3	157.8	−42.5	noHB	1.945 Å(140.0°)C	7.85
b**X11**	−175.7	−121.2	−19.2	153.8	−45.3	noHB	1.983 Å(138.3°)C	7.89
b**X12**	−158.4	130.8	31.3	130.5	−39.0	2.174 Å(169.8°)thia	1.999 Å(140.1°)C	8.11
b**X13**	−158.5	−115.9	−7.2	32.1	−165.9	1.994 Å(143.0°)EE	noHB	9.43

dx.doi.org/10.1021/jp212628v | J. Phys. Chem. B 2012, 116, 7605−7617

Table 1. continued

	torsional angles					hydrogen bond distances and angles[d,e]		
	epoxide 10−11−12−O12	side chain 14−15−16−17	side chain 16−17−18−19	3-hydroxyl 2−3−O3−H3	7-hydroxyl 6−7−O7−H7	3-hydroxyl	7-hydroxyl	MP2 energies[f]
b**X14**	75.9	−119.8	−13.6	−79.4	−168.7	1.920 Å(138.1°)C	noHB	10.07
b**X15**	−165.7	−122.4	174.8	80.6	−168.7	*2.495 Å(114.2°)EC*	noHB	10.11
b**X16**	−179.7	−120.9	−13.7	−87.1	70.4	1.936 Å(140.5°)C	noHB	10.43
b**X17**	−170.9	−118.0	−16.4	−91.3	−176.6	1.871 Å(143.3°)C	noHB	10.62
b**X18**	−164.1	−117.5	−10.8	81.4	−168.3	*2.513 Å(113.5°)EC*	noHB	10.69
b**X19**	96.8	−116.4	−12.1	158.2	−40.4	noHB	1.942 Å(140.5°)C	10.70
b**X20**	−177.2	63.9	20.9	−81.4	73.5	1.924 Å(138.5°)C	noHB	11.07
b**X21**	79.3	−118.5	−12.9	156.3	−33.7	noHB	1.977 Å(141.4°)C	11.34
b**X22**	68.5	−121.0	−17.8	171.6	−168.1	*2.922 Å(93.6°)C*	noHB	11.50
b**X23**	−165.1	−118.2	−15.5	160.5	−140.8	noHB	2.162 Å(152.5°)EE	11.93
b**X24**	−166.1	−122.0	−17.6	151.0	83.1	noHB	2.401 Å(131.1°)EE	12.35
b**X25**	−170.1	−121.2	−19.3	152.9	−164.5	noHB	noHB	12.80
b**X26**	178.0	−116.2	−14.7	−82.7	−168.0	1.893 Å(140.4°)C	noHB	12.88
b**X27**	−153.2	131.2	31.7	137.7	−179.9	2.227 Å(166.4°)thia	noHB	13.03
b**X28**	−151.9	−117.0	−16.2	153.8	−171.2	noHB	noHB	13.64
b**X29**	−141.4	−119.3	−16.8	−144.9	−173.3	2.030 Å(131.4°)C	noHB	14.62
b**X30**	172.7	−115.2	−12.6	−95.5	76.3	1.902 Å(142.4°)C	noHB	15.18
b**X31**	162.9	−120.3	−17.5	51.9	−174.9	2.049 Å(137.0°)EC	noHB	15.53
b**X32**	−154.3	−120.2	−18.4	153.8	−172.8	noHB	noHB	17.65
b**X33**	−60.5	−121.5	−16.5	171.7	−171.5	*2.948 Å(92.0°)C*	noHB	18.01
b**Y01**	51.6	−105.3	−0.9	60.2	−165.9	2.075 Å(130.8°)EE	noHB	7.03
b**Y02**	8.9	−102.2	−0.3	79.1	−171.3	*2.746 Å(112.0°)EE*	1.892 Å(163.2°)epo	7.20
b**Y03**	7.5	77.5	−29.8	−81.2	71.9	1.910 Å(139.2°)C	noHB	7.54
b**Y04**	29.7	115.0	21.4	59.6	−53.8	*2.263 Å(119.5°)EC*	2.090 Å(134.1°)C	8.12
b**Y05**	−160.9	−100.1	13.4	73.1	−163.0	*2.408 Å(119.2°)EE*	noHB	9.51
						2.587 Å(148.9°)epo		
b**Y06**	0.9	84.4	−27.3	−72.9	−34.8	1.975 Å(134.9°)C	2.039 Å(140.1°)C	9.55
b**Y07**	34.7	106.5	−10.2	−38.6	71.9	*2.614 Å(107.0°)EE*	noHB	11.92
						1.999 Å(160.3°)epo		
						2.968 Å(101.1°)C		
b**Y08**	18.5	−96.8	10.7	67.5	79.2	*2.488 Å(119.2°)EE*	noHB	11.96
b**Y09**	31.4	−103.1	4.9	57.1	71.4	2.077 Å(133.0°)EE	noHB	12.43
b**Y10**	7.6	−91.3	15.6	40.3	−164.5	2.018 Å(141.6°)EC	noHB	12.58
b**Y11**	−178.1	−98.7	12.7	63.9	−160.7	2.155 Å(128.7°)EE	noHB	13.46
b**Y12**	11.7	−104.1	−13.8	53.7	67.9	*3.057 Å(117.2°)EE*	1.919 Å(158.9°)O3	15.06
						1.871 Å(170.5°)epo	*3.139 Å(90.1°)C*	
b**Y13**	−17.4	80.3	−28.9	−67.0	77.5	2.013 Å(131.4°)C	noHB	15.89
b**Y14**	28.7	114.4	19.8	137.1	70.6	*2.587 Å(104.3°)C*	noHB	16.13

[a]deg. [b]Å, deg. [c]kcal*mol^{-1}. [d]Specific electrostatic interaction rather than hydrogen bonding are italic;. [e]Hydrogen bonding to C, O atom of ketone; EC, carbonyl O atom of ester; EE, noncarbonyl O atom of ester; epo, O atom of epoxide; thia, N atom of thiazole; noHB, lack of hydrogen bonding. [f]Absolute energies in Hartrees are given in Table SI1.

dx.doi.org/10.1021/jp212628v | J. Phys. Chem. B 2012, 116, 7605−7617

Table 2. Selected Torsion Angle Values[a], Hydrogen Bond Parameters[b], and Correlated Energy Correction (MP2) Relative Energies[c] for Stable DFT Conformations of Ixabepilone at the MP2/6-31+G(d,p)//B3LYP/6-31+G(d,p) Level of Theory

	torsional angles					hydrogen bond distances and angles[d,e]			
	epoxide 10−11−12−O12	side chain 14−15−16−17	side chain 16−17−18−19	3-hydroxyl 2−3−O3−H3	7-hydroxyl 6−7−O7−H7	3-hydroxyl	7-hydroxyl	N−H	MP2 energies[c,f]
iH01	−177.3	−118.7	179.8	63.6	−166.8	2.045 Å(132.0°)AC	noHB	noHB	6.32
iH02	−176.5	115.1	13.0	63.2	−82.4	2.042 Å(132.2°)AC	noHB	noHB	6.66
iH03	−177.9	−122.3	−18.8	64.0	−83.3	2.063 Å(131.4°)AC	noHB	noHB	7.04
iH04	−178.6	−123.9	175.7	160.0	−168.4	noHB	noHB	noHB	7.65
iH05	−174.4	108.7	−177.0	61.3	−82.4	2.001 Å(133.8°)AC	noHB	noHB	7.69
iH06	−177.9	100.3	−16.2	158.8	−82.1	noHB	noHB	noHB	8.15
iH07	−178.4	95.2	−179.4	160.2	−167.7	noHB	noHB	noHB	8.45
iH08	−177.8	94.6	−179.5	158.0	−83.3	noHB	noHB	noHB	8.58
iH09	−177.9	−117.5	−16.8	156.4	−83.7	noHB	noHB	noHB	8.74
iM01	−171.0	107.2	27.1	133.7	−163.0	2.129 Å(162.7°)thia	noHB	noHB	4.58
iM02	−155.4	−109.5	20.2	168.2	−168.7	noHB	noHB	2.125 Å(132.1°)O3	5.21
iM03	−173.8	87.1	−179.0	42.6	−160.6	1.954 Å(142.5°)AC	noHB	noHB	5.27
iM04	−172.9	−122.0	174.5	38.2	−160.2	1.966 Å(143.5°)AC	noHB	noHB	5.29
iM05	−152.6	1.7	−13.9	166.4	−168.0	noHB	noHB	2.206 Å(128.1°)O3	5.81
iM06	−173.6	−110.8	−12.1	41.7	−84.3	1.934 Å(143.0°)AC	noHB	noHB	5.94
iM07	−174.7	−102.9	15.7	44.0	−161.9	1.933 Å(142.3°)AC	noHB	noHB	6.25
iM08	−174.1	−110.5	−11.4	42.6	−160.2	1.947 Å(142.5°)AC	noHB	noHB	6.31
iM09	−152.0	−0.9	176.3	165.8	−168.7	noHB	noHB	2.225 Å(127.4°)O3	6.40
iM10	−158.0	−111.0	19.3	−63.5	−167.4	noHB	noHB	2.072 Å(135.7°)O3	6.44
iM11	−165.4	114.6	−23.8	170.7	−167.5	noHB	noHB	2.055 Å(134.3°)O3	6.93
iM12	−172.8	163.9	−34.1	140.6	165.5	2.142 Å(156.1°)thia	noHB	noHB	7.13
iM13	−161.2	116.8	−177.1	−63.7	−166.8	noHB	noHB	2.064 Å(135.8°)O3	7.30
iM14	−174.7	−109.5	−11.8	42.2	69.6	1.925 Å(143.0°)AC	noHB	noHB	7.53
iM15	−174.0	30.7	178.9	−60.1	−167.6	noHB	noHB	2.015 Å(137.0°)O3	8.10
iP01	−171.3	−139.7	−132.2	89.2	−43.6	2.081 Å(159.8°)thia	1.947 Å(139.6°)C	noHB	0.89
iP02	−174.1	103.9	31.6	119.1	−44.0	2.057 Å(172.7°)thia	1.948 Å(139.5°)C	noHB	1.34
iP03	−142.6	−99.7	177.0	35.3	−41.4	1.934 Å(144.4°)AC	1.957 Å(139.5°)C	noHB	1.59
iP04	122.7	80.7	−24.6	36.5	−45.8	2.004 Å(143.0°)AC	1.941 Å(139.0°)C	noHB	4.13
iP05	123.2	83.4	−178.3	35.2	−45.8	2.004 Å(143.2°)AC	1.943 Å(139.0°)C	noHB	4.76
iP06	115.8	−100.9	19.1	38.9	−46.9	1910 Å(143.9°)AC	1.960 Å(138.3°)C	noHB	4.94
iP07	117.7	−100.2	178.4	36.7	−46.4	1.941 Å(143.9°)AC	1.949 Å(138.6°)C	noHB	5.26
iP08	−144.4	30.6	177.3	174.0	−47.5	noHB	2.129 Å(135.0°)C	2.227 Å(129.8°)O3	6.43
iP09	114.1	27.3	178.1	174.1	−48.7	noHB	2.092 Å(135.4°)C	2.184 Å(130.5°)O3	7.17
iP10	115.4	7.4	15.3	−16.5	−46.2	2.304 Å(141.3°)AC	1.949 Å(138.6°)C	noHB	8.74
iP11	113.3	5.0	175.8	10.5	−46.7	2.416 Å139.2(°)AC	1.959 Å(138.3°)C	noHB	9.15
iN01	26.6	122.0	19.0	58.6	−49.3	1.957 Å(135.6°)AC	1.943 Å(138.0°)C	*2.327 Å(113.8°)epo*	4.35
iN02	26.5	127.6	−173.7	59.4	−50.4	1.969 Å(135.1°)AC	1.948 Å(137.6°)C	*2.279 Å(117.3°)epo*	4.36
iN03	33.0	−6.2	−16.2	−68.0	−58.5	2.247 Å(128.5°)C	2.167 Å(130.2°)C	*2.271 Å(120.1°)epo*	8.85
iN04	32.9	−9.5	173.8	−67.6	−58.2	2.275 Å(128.0°)C	2.155 Å(130.6°)C	*2.333 Å(115.8°)epo*	9.33
iS01	31.5	95.9	−179.7	−78.4	−58.0	1.980 Å(136.7°)C	2.019 Å(132.6°)C	2.089 Å(129.7°)epo	4.76
iS02	32.4	109.9	13.2	−79.4	−57.9	1.984 Å(137.0°)C	2.024 Å(132.7°)C	2.057 Å(132.0°)epo	4.88

dx.doi.org/10.1021/jp212628v | J. Phys. Chem. B 2012, 116, 7605−7617

Table 2. continued

	torsional angles					hydrogen bond distances and angles[d,e]			
	epoxide 10−11−12−O12	side chain 14−15−16−17	side chain 16−17−18−19	3-hydroxyl 2−3−O3−H3	7-hydroxyl 6−7−O7−H7	3-hydroxyl	7-hydroxyl	N−H	MP2 energies[c,f]
iS03	31.2	−87.5	25.6	−79.5	−57.7	1.970 Å(137.0°)C	2.005 Å(133.0°)C	2.188 Å(125.5°)epo	5.58
iS04	31.1	−87.1	175.1	−79.4	−57.6	1.975 Å(137.0°)C	2.002 Å(133.2°)C	2.145 Å(128.5°)epo	6.26
iT01	−174.1	84.3	−22.8	37.3	−46.0	2.019 Å(142.3°)AC	1.950 Å(138.6°)C	noHB	2.00
iT02	−176.7	−99.3	21.6	34.7	−46.5	1.934 Å(144.0°)AC	1.957 Å(138.2°)C	noHB	4.41
iT03	123.7	84.3	−178.3	34.7	−45.7	2.010 Å(143.2°)AC	1.942 Å(139.0°)C	noHB	4.78
iT04	117.7	−109.0	172.7	37.2	−46.7	1.937 Å(143.9°)AC	1.954 Å(138.4°)C	noHB	4.82
iW01	1.0	95.8	−25.4	119.4	−168.0	2.078 Å(138.3°)epo	noHB	2.143 Å(126.9°)O3	0.19
iW02	0.1	92.6	−177.6	116.3	−168.7	2.026 Å(142.0°)epo	noHB	2.200 Å(123.8°)O3	0.37
iW03	0.3	−95.8	18.1	118.5	−167.7	2.037 Å(140.8°)epo	noHB	2.171 Å(126.4°)O3	1.52
iW04	0.1	−89.6	177.9	119.7	−167.1	2.057 Å(139.3°)epo	noHB	2.146 Å(128.1°)O3	1.61
iX01	−139.4	108.7	30.3	115.9	−41.6	2.095 Å(174.3°)thia	1.984 Å(139.1°)C	noHB	0.00
iX02	−174.1	105.6	29.5	119.3	−44.2	2.065 Å(172.6°)thia	1.951 Å(139.3°)C	noHB	1.43
iX03	−177.1	−103.2	176.2	34.9	−46.3	1.979 Å(143.4°)AC	1.954 Å(138.4°)C	noHB	4.25
iX04	−154.1	−128.5	177.6	−106.7	−174.8	1.785 Å(147.1°)C	noHB	noHB	4.26
iX05	175.0	160.2	−32.8	133.3	−45.4	2.062 Å(161.7°)thia	1.958 Å(138.8°)C	noHB	4.93
iX06	−175.8	66.9	23.8	−82.2	−45.5	1.992 Å(137.3°)C	1.975 Å(137.7°)C	noHB	5.13
iX07	−155.3	−120.3	−14.7	−59.3	−52.0	2.037 Å(132.5°)AC	1.950 Å(137.4°)C	noHB	5.53
						2.533 Å(107.5°)C			
iX08	−172.7	−123.1	173.4	−84.3	−166.2	1.927 Å(139.7°)C	noHB	noHB	5.62
iX09	−166.8	−112.9	176.6	74.6	−168.4	*2.373 Å(119.9°)AC*	noHB	noHB	8.30
iX10	−153.4	−118.3	−19.7	159.7	−46.5	noHB	2.052 Å(136.8°)C	noHB	8.32
iX11	−164.4	−115.5	−13.0	75.9	−168.4	*2.415 Å(118.7°)AC*	noHB	noHB	8.56
iX12	−159.9	137.4	29.7	123.3	−38.0	2.160 Å(174.3°)thia	1.978 Å(140.6°)C	noHB	8.79
iX13	−153.5	−118.4	−10.7	164.8	−94.9	noHB	1.837 Å(160.2°)AC	*3.137 Å(105.0°)O3*	8.98
							3.135 Å(90.2°)C		
iX14	−163.2	−121.6	−20.0	67.5	−162.7	2.145 Å(127.2°)AC	noHB	noHB	9.10
iX15	73.7	−103.9	14.4	−78.2	−166.2	1.938 Å(136.9°)C	noHB	noHB	10.55
iX16	−153.8	−100.4	20.5	42.2	−170.5	2.063 Å(140.6°)AC	noHB	noHB	10.70
iX17	180.0	77.4	−23.8	−80.4	72.0	1.947 Å(137.7°)C	noHB	noHB	10.86
iX18	−172.6	−115.3	−16.3	−94.4	−164.5	1.873 Å(144.1°)C	noHB	noHB	11.01
iX19	176.4	−101.0	18.2	−85.8	65.8	1.943 Å(139.8°)C	noHB	noHB	11.04
iX20	4.8	−119.5	−15.0	161.1	−41.6	noHB	1.955 Å(140.0°)C	noHB	11.34
iX21	74.4	−118.6	−20.2	164.0	−167.3	noHB	noHB	noHB	11.70
iX22	93.8	−113.5	−11.8	166.3	−41.1	noHB	1.949 Å(140.1°)C	noHB	12.97
iX23	−167.2	−115.4	−22.3	151.3	−162.1	noHB	noHB	2.165 Å(173.5°)O7	13.16
iX24	81.8	−114.7	−14.8	164.3	−32.3	noHB	1.971 Å(141.8°)C	noHB	13.23
iX25	−142.5	−114.9	−18.1	−179.4	−169.1	*2.555 Å(104.8°)C*	noHB	noHB	13.77
iX26	−170.1	−115.5	−14.9	−154.8	−159.9	2.096 Å(125.2°)C	noHB	noHB	13.98
iX27	104.0	−117.6	−18.8	47.1	−173.0	1.914 Å(139.5°)AC	noHB	noHB	14.45
iX28	98.3	−127.2	18.3	−90.1	82.7	1.785 Å(144.8°)C	noHB	1.889 Å(140.9°)O3	15.09
iX29	−156.0	137.4	28.3	132.5	−175.4	2.161 Å(168.0°)thia	noHB	noHB	15.46
iX30	−69.0	−116.0	22.0	157.8	−170.5	noHB	noHB	noHB	19.14

dx.doi.org/10.1021/jp212628v | J. Phys. Chem. B 2012, 116, 7605−7617

Table 2. continued

	torsional angles					hydrogen bond distances and angles[d,e]			
	epoxide 10−11−12−O12	side chain 14−15−16−17	side chain 16−17−18−19	3-hydroxyl 2−3−O3−H3	7-hydroxyl 6−7−O7−H7	3-hydroxyl	7-hydroxyl	N−H	MP2 energies[c,f]
iX31	−159.0	−121.2	−18.9	160.6	−170.1	noHB	noHB	noHB	21.53
iY01	35.3	110.1	16.5	66.1	−54.2	noHB	2.047 Å(134.4°)C	2.266 Å(128.7°)epo *2.220 Å(118.4°)O3*	4.62
iY02	29.6	123.8	20.6	60.3	−54.5	2.271 Å(123.8°)AC	2.117 Å(133.4°)C	*2.819 Å(105.1°)epo*	5.07
iY03	−150.9	−93.4	24.6	122.0	−162.4	2.168 Å(155.6°)epo	noHB	*2.926 Å(104.1°)epo* 2.221 Å(127.1°)O3	5.16
iY04	15.4	99.1	−22.0	−79.1	69.6	1.949 Å(138.0°)C	noHB	2.060 Å(131.9°)epo	5.66
iY05	5.2	−94.9	17.6	168.8	155.5	noHB	2.161 Å(163.5°)epo	2.093 Å(134.3°)O3	6.09
iY06	50.2	−98.6	12.3	−58.4	−168.5	noHB	noHB	2.021 Å(136.7°)O3	6.26
iY07	4.1	−92.0	24.0	−39.0	−162.3	*3.130 Å(103.8°)AC*	noHB	2.036 Å(136.1°)epo	6.64
iY08	23.5	91.7	−27.5	−72.7	−36.1	1.992 Å(134.4°)C	2.014 Å(139.9°)C	2.170 Å(127.2°)epo	7.16
iY09	14.3	−95.0	20.1	115.6	50.9	2.001 Å(144.5°)epo	noHB	2.202 Å(125.1°)O3	7.75
iY10	37.0	119.4	17.2	−38.3	71.1	2.095 Å(160.2°)epo *2.924 Å(101.7°)C*	noHB	2.325 Å(121.3°)epo	9.40
iY11	23.2	−92.9	17.0	−52.2	82.2	noHB	noHB	*2.877 Å(98.1°)epo* 2.151 Å(135.9°)O3	11.94
iY12	12.5	−106.7	−12.2	56.9	68.5	1.923 Å(164.9°)epo	1.923 Å(159.7°)O3	noHB	13.34
iY13	176.8	−95.5	18.2	47.8	−158.4	noHB	noHB	2.130 Å(130.0°)epo *2.766 Å(101.6°)O3*	13.95
iY14	−12.6	92.1	−27.3	−77.6	69.6	1.958 Å(137.2°)C	noHB	2.208 Å(125.1°)epo	16.02

[a]deg. [b]Å, deg. [c]kcal*mol^{-1}. [d]Specific electrostatic interaction rather than hydrogen bonding are italic. [e]Hydrogen bonding to C, O atom of ketone; AC, carbonyl O atom of amide; O3, O atom of 3-hydroxyl; O7, O atom of 7-hydroxyl; epo, O atom of epoxide; thia, N atom of thiazole; noHB, lack of hydrogen bonding. [f]Absolute energies in Hartrees are given in Table SI6.

dx.doi.org/10.1021/jp212628v | J. Phys. Chem. B 2012, 116, 7605−7617

solution, the default integral equation formalism polarizable continuum model (IEF-PCM)[50] with full geometry optimization was employed at the PCM/MP2/6-31+G(d,p)//PCM/B3LYP6-31+G(d,p) level.

RESULTS AND DISCUSSION

A Structural Comparison of Epothilone A and Patupilone. The transformation of the structure of epothilone A into patupilone (epothilone B) formally relies on the substitution of a methyl group for the hydrogen atom at the tetrahedral bridging C12 atom of the epoxide. The chirality does not change, and this substitution usually has no effect on the conformations of the macrolactone ring. Interestingly, for the endo **W** subset,[45] all the conformers corresponding to epoA and epoB (Table SI2, Supporting Information) have essentially identical macrocyclic rings. In some rare cases, however, especially in structures that contain no more than one intramolecular hydrogen bond, the torsional deformation is considerable (more than 0.3 Å rms deviation of ring atoms) but spreads out over the entire macrocycle. An example of this type of exception is structure b**X28**,[41] (Table 1), which has no intramolecular hydrogen bonds and has rms deviations of 0.40 Å for its epoA and epoB conformers. Similarly, structures such as b**H01**[2] and b**X29**, which have only a 3-OH → O═C5 hydrogen bond, have rms deviations between the macrocyclic atoms of 0.55 Å and 0.47 Å, respectively. Additionally, b**Y11**[41] contains only a 3-OH → O−C1 hydrogen bond and has an rms deviation of 0.45 Å. I found only two examples of distorted macrocycle geometries (b**P03**[43] and b**N04**[18]) in which two hydrogen bonds were present. The formation of an additional hydrogen bond, especially if it is transannular, occurs with a significant conformational change in the ring. For example, an epoA analogue of virtual b**X24**[41] exhibits a good hydrogen bonding geometry from 7-OH → O═C5 (2.065 Å, 131.4°), but the patupilone analogue b**X24** adopts a 7-OH → O−C1 pattern (2.401 Å, 131.1°). This transannular interaction causes a total distortion of the former conformation of the macrocycle. Similarly, I observed that the replacement of the ester group by an amide does not change the overall molecular shape unless the hydrogen bond pattern also changes.

In particular, the C10−C11−C12−O12 torsion is the most significant parameter for defining the exo−endo type of conformation (Table 1 and 2). These epothilone structures possess two (patupilone) or three (ixabepilone) intramolecular hydrogen bonds that stabilize and fully control their macrocyclic conformations, which are even independent of lactone−lactam structural change. However, sometimes this change may cause the reorganization of the existing hydrogen bonds, leading to the subsequent distortion of the ring. The cases reported below are clearly in this category. Endo conformers b**N04** and i**N04** (or b**Y10** and i**Y07**), which have rms deviations of 0.60 Å and 0.49 Å, respectively, are helpful illustrations of the former, while b**Y05** and i**Y03** illustrate the latter hydrogen bond reconfiguration. However, the rms deviation never exceeds 0.6 Å. (Figure SI1).

Conformational Analysis of Patupilone. The global minimum for the conformer set of epothilone B, using both DFT and MP2 methods, is represented by structure b**P01** (Table 1, Figure 1), which reveals a strong intramolecular hydrogen bond between the 3-hydroxyl and the thiazole ring. All the compact structures that were found[42] produced the same rank ordering of the energies, although the correlation method predicts an equilibrium between experimental

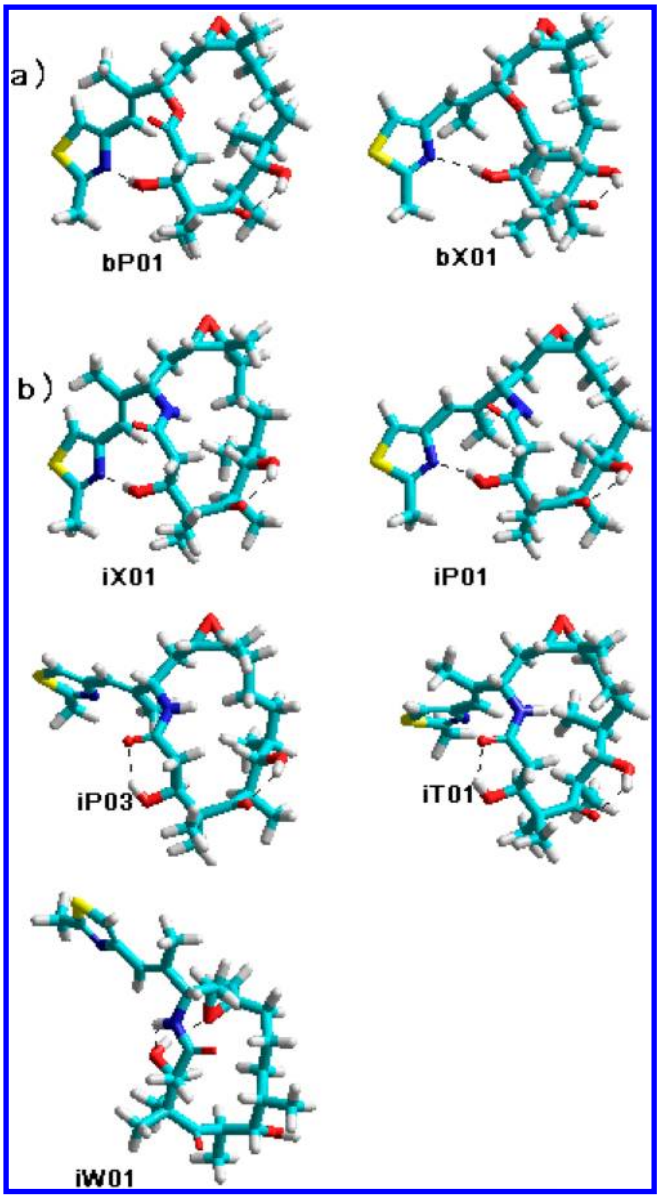

Figure 1. Tube models of the most stable representative conformations of (a) patupilone, (b) ixabepilone.

structures b**P01** and b**P02** and virtual structure b**X01** (99% of total population from the Boltzmann distribution; Table SI1), whereas B3LYP shows a simple preference for one conformer. The hydrogen bonds from 3-OH to the thiazole ring and from 7-OH to the ketone carbonyl are marked features of the most stable epothilone B conformers. These structures dictate their compact shape[42] and appear to account fairly well for the total energy of the molecule. It is not astonishing that the most stable structure, b**P01**, has the shortest 3-OH hydrogen bond (2.039 Å), whereas b**X27**, which is less stable by 13 kcal/mol, has the longest hydrogen bond (2.227 Å) (Table 1). With one exception, all the hydrogen bonds are only weakly bent due to the flexible character of the eleven-membered bridge, resulting in angles that exceed 160°. It should be mentioned that the typical trans geometry of the lactone group is distorted away from planarity (by 13−20°; TableSI3), likely as the $\pi-\pi$ alkene−thiazole conjugation of the side-chain (by an angle of 31−48°; Table 1).

dx.doi.org/10.1021/jp212628v | J. Phys. Chem. B 2012, 116, 7605−7617

My study corroborates the importance of the basic nitrogen atom that is found at the 2′-position in both natural epothilones[51] and synthetic analogues that contain a heterocyclic side chain.[52] It has been established previously that there are some requirements for the specific positioning of this nitrogen atom.[53,54] The crowded nature of some analogues with heterocyclic substituents may make it difficult to fit into the tubulin receptor, but it may also hinder the formation of a compact conformation.[55] The considerable activity of flat benzothiazole epothilones in the induction of tubulin polymerization[56,57] suggests that both processes have some flexibility with respect to the torsion of the aromatic ring.

The presence of three abundant conformers in a dynamic equilibrium at room temperature was suggested by vacuum calculations. The populations of the two conformers b**P01** and b**P02** are not controlled by the side-chain torsion angle C14−C15−C16−C17; instead, the hydrogen bond from the 3-hydroxyl to the nitrogen atom of the thiazole is the dominant factor. The differences between energy levels and relevant geometric parameters of b**P02** and virtual structure b**X01** (third in the energy order) are negligible. The macrocycle of conformer b**X01** is quite similar to that of the conventional b**P** subset: the ring methylene chain modification is limited to the C8−C13 region (Table SI2).

Two other compact conformers, b**M01** and b**M02**,[29] are appreciably higher in energy and have a different 16-membered-ring folding pattern in the regions of both the carbonyl and the 7-hydroxyl group.[42] For compact b**M** structures, intramolecular hydrogen bonding between these two partners is uncommon, and this may be responsible for the reduced stability. Special attention should be paid to b**X12**, a compact structure that is less stable than the global minimum by approximately 8 kcal/mol, even though the overall structural picture of the functionalized part of the molecule is essentially the same as that of the most stable structure, b**P01** (Table 1, Figure SI2). A small, destabilizing conformational change between the ester group and the oxirane ring occurs as the torsional angle in the C13−C15 region is modified. This local change, which allows the side chain to reach an overall compact conformation, is no longer found in the families of the epothilone and ixabepilone conformers examined here (conformer b**X27** is referred to here as the 7-hydroxyl rotamer of b**X12**). This change causes a transannular steric interaction between the H(C3) and H(C17) hydrogen atoms (r = 2.08 Å) and a stereoelectronic effect between the lone pairs on the oxirane oxygen atom and the electron-rich double-bond π orbitals (O−C distances are only about 3.0 and 3.8 Å).

An interesting related issue involves virtual structures that have basically the same pattern of hydrogen bonding but yield differences in energies. Examples of such pairs of structures can be found between both the exo and endo conformer sets (Table 1). The exo structure b**X22**, which has a hydrogen bond contact and differs somewhat from b**X33** only in the arrangement of the C9−C11 region, is more conformationally stable by 6.5 kcal/mol. This may be explained by the unfavorable C10−C11−C12−C13 torsional change (ac to sp for b**X33**; Table SI2, Figure SI2) and the strengthening of the transannular interactions that are derived from direct contacts between macrocycle hydrogen atoms. Structure b**X33** contains two nonbonded steric interactions between methylene hydrogens at C10 and the hydrogen at C14 (2.25 Å and 2.34 Å) instead of the one interaction (2.22 Å) found in b**X22**. Additionally, the functionalized part of the macrocycle is made more crowded, where the distances to H(C2) and H(C6) are 2.14 Å and 2.22 Å, respectively. The 6.6 kcal/mol difference in energy between b**H04** and b**X29** may also not be attributable to unfavorable changes in the C8−C9−C10−C11 torsion (ap to sc) (Table SI2, Figure SI2), because two destabilizing transannular interactions (2.12 Å from H(C2) to H(C6) and 2.19 Å from H(C2) to H(C9)) are observed in the more stable conformer, and no transannular interactions involving hydrogen atoms are seen in its more stable counterpart. The only explanation appears to be the strong repulsive interaction between H(C10) and the O(C1) atom. Similarly, the 5.5 kcal/mol of torsional strain in the C5−C7 and C10−C12 fragments (Table SI2, Figure SI2) only partly clarifies the instability of b**X25** compared to b**X09**. For conformer b**X25**, the distances of the H(C2)−H(C6) and H(C11)−H(C14) nonbonded hydrogen−hydrogen interactions (1.93 Å and 2.09 Å, respectively) are substantially shorter than the corresponding distances for b**X09** (2.18 Å and 2.27 Å, respectively). For comparison, the sum of the van der Waals radii for two hydrogen atoms is 2.40 Å.[58]

Representative examples in which the structural dependence of a local destabilizing torsional strain forces and transannular steric repulsions are also found in the endo series, and their energetic consequences are presented quantitatively in Table 1 (cf. b**Y01** and b**Y08**, b**Y03** and b**Y13**, and b**W04** and b**Y10** pairs of conformers (Figure SI3)).

A systematic survey of all the experimental conformers of the macrolide scaffold of epothilone A has been recently completed.[42] An ab initio potential energy surface for epothilone B is currently available, and the remarkable congruence of the conformers found for epothilones A and B indicates that the previous assessment of factors contributing to the overall stability of the molecule provides a complete picture. The hydrogen bond between the 3-hydroxyl group and the side-chain thiazole plays a key role in structural determination and allows the identification of stable compact conformer sets even across three different macrocyclic scaffolds. Other structures from the exo b**P**[43] set, which probably have the most relaxed macrocycles among the conformers of patupilone,[42] are not stable enough to compete, even though they have short intramolecular hydrogen bonds between the 3- and 7-hydroxyl groups and the ester and ketone carbonyls, respectively. Note that the compact conformers are formed exclusively as exo structures; endo structures are unable to cluster for steric reasons. The most stable endo conformer, b**W01**, is also too unstable to represent the endo series in the conformer mixture. As may be anticipated, the bifurcated hydrogen bond from 3-OH to both the oxirane and the noncarbonyl ester oxygen atom has little impact on the overall conformational stability. A collection of virtual structures that completes the accessible conformational space of the molecule offers convincing evidence that the exo (**X**) and endo (**Y**) groups, with two exceptions (b**X01** and b**X02**), represent two sets of relatively unstable structures. Relative to the global minimum, energies can range from approximately 5 to 18 kcal/mol for exo structures and 7 to 16 kcal/mol for endo conformers. A possible explanation for these high-energy structures is that they are structurally unable to form hydrogen bonds (b**X25**, b**X28**, b**X32**) or able to form only poor hydrogen bond contacts (b**X22**, b**X33**). The unfavorable torsional (Table SI2) and transannular steric interactions may also contribute, although this is not more important than the hydrogen-bonding factors (Table 1). In summary, a detailed conformational

dx.doi.org/10.1021/jp212628v | J. Phys. Chem. B 2012, 116, 7605−7617

analysis of patupilone (epothilone B) leads to the same conclusions as our recent studies of epothilone A[42] and predicts very similar conformational profiles for these two compounds.

Conformational Analysis of Ixabepilone. There are four types of hydrogen bonds that are commonly formed in ixabepilone conformers; NH → O−C3 and 3-OH → O═C1 are very common, but NH → epoxide and 3-OH → epoxide bonds are also possible in the endo form due to the natural proximity of NH proton donor to the epoxide and the considerable basicity of its oxygen (Table 2). The conformational analysis of ixabepilone yielded three distinct types of stable conformers that can be classified according to their hydrogen bonding patterns (Figure 1). The exo series is represented by two types of structures in which both hydroxyl groups act as proton donors, but the NH group is not engaged. Both of these structural types have hydrogen bonds between 7-OH and the ketone. The compact structures in which the 3-hydroxyl hydrogen bonds with the thiazole ring (i**X01**, i**X02** and i**P01**, i**P02**) are more stable than those in which the amide carbonyl acts as a proton acceptor (i**P03**−i**P07** and i**T01**−i**T04**; Table 2). In the endo series, structural features exclude the 7-OH from consideration, but the NH donor may interact with the proximal 3-hydroxyl, which strongly interacts with the epoxide (Figure 1). This cooperative mechanism[59] is evidently so effective that all the i**W** conformers are stable enough to coexist with those of the exo series. Note (*vide supra*; Table 1) that the 3-hydroxyl group of b**W** participates in a bifurcated hydrogen bond that fully exploits neighboring proton acceptors in the same way as i**W**, where the transformation from an ester group into an amide allows for an additional (and cooperative) hydrogen bond to be formed (Table 2). The unique functional environment of the lactam provides the framework for an extensive hydrogen bonding network that can very effectively stabilize the ixabepilone system. Thus, it is evident that a "point mutation" that exchanges the oxygen atom in the macrocycle ester for an NH group paves the way for the endo series to energetically compete with exo structures for the taxol binding site. My results are consistent with the recent literature[35] and confirm the real, significant conformational variety of ixabepilone compared to the more homogeneous structural landscapes of patupilone and epothilone A.

This seemingly minor structural modification of epothilone B, in which the ester is transformed into an amide, leads to an unexpectedly large change in the conformational profile of ixabepilone; although compact structures are still important, they are not the only stable conformers. Exchanging the ester for an amide has pronounced effects on the compound's ability to form hydrogen bonds. On the one hand, there is an obvious, but remarkable, increase in the proton-accepting ability of the amide carbonyl, in which the partial negative charge on the oxygen atom is greater than that of the carbonyl oxygen atom in the ester group (NBO charges are −0.737 and −0.708 for *N*-methylacetamide and methyl acetate, respectively). As a result, the two similar structures i**P03**[43] and i**T01**[44] are only 1.5 to 2.0 kcal/mol less stable than the global minimum due to the strength of the 3-OH → O═C1 and 7-OH → O═C5 hydrogen bonds (Table 2). On the other hand, in the endo series, the strong proton-donor group NH has close contact with the oxygen atom of the epoxide (subsets i**N** and i**S**) or with the O3 oxygen (subset i**W**). However, all the presented i**N** and i**S** conformers that use the proton-donor characters of NH and both hydroxyl groups to form three short hydrogen bonds (r = 1.95 − 2.3 Å) (Table 2) are not stable, probably because of significant torsional effects in the macrocycle.[42] Meanwhile, the geometry of the macrocycle scaffold in the i**W** subset allows for the facile development of hydrogen bonding from the proton donor NH to the 3-OH oxygen atom, which in turn extends to the oxirane ring (the NBO charge for the oxygen atom in 1,1,2-trimethyloxirane is −0.651). The cooperative hydrogen bonds found in the i**W** subset enhance the overall hydrogen bonding of the system and contribute significantly to the total energy gain; the most stable ixabepilone species are i**W** conformers (the Boltzmann population of the i**W** conformers is 48.0%; Table SI6) (Figure 1). It is worth noting that a NH → O−C3 interaction is present among i**M** and i**P** conformers, sometimes with a more favorable geometry (i**M**), but 3-OH cannot act as a proton donor for structural reasons; thus, there is no extra stabilization provided to the system by cooperative hydrogen bonding.

The four most stable compact structures (two i**P** and two i**X** conformers) found in this study, including the global minimum, have energies of approximately 1.5 kcal/mol (a population of 48.3% is calculated; Table SI6). All the structures contain short 3-OH → thiazole hydrogen bonds (r < 2.1 Å) that adopt a nearly linear geometry (only one structure, i**P01**, has an angle smaller than 170°). This favorable geometry is achieved at the expense of an increased tilt to the amide bond (the out-of-plane peptide tilt in the range of 15−24° is higher than in the patupilone compact counterparts; Table SI8) and less effective π-conjugation in the side chain (the dihedral angle between the thiazole and the adjacent double bond varies over the range of 30−48°; Table 2).(cf.56,57) The internal 7-OH → O−C5 hydrogen bond (with optimal parameters, r < 2.0 Å and the O7−H···O5 angle ca. 140°) is probably the main additional intrinsic stabilizing factor that contributes to the relatively low energy of the compact conformers of ixabepilone. The conformers i**M01** and i**M12**, which possess nearly identical 3-OH to thiazole hydrogen bonds, are much less stable than i**X01** (by 4.6 and 7.1 kcal/mol, respectively) because of, *inter alia*, the lack of any contribution from NH or 7-OH hydrogen bonding. i**X05** and i**X12**, two other compact conformers that have the same pattern of hydrogen bonds as i**X01**, exhibit bad nonbonded contacts that are not observed in i**X01** (H(C2)−H(C7) and H(C7)−H(C10) for i**X05**; H(C3)−H(C17) and H(C7)−H(C10) for i**X12**) (Figure SI4).

Two examples of compact conformers illustrate how the close proximity of functional groups within the molecule results in the stereoelectronic control of its stability. It is intriguing that the conformer i**X05**, which has the same pattern of hydrogen bonds as i**P01** and an rms deviation for all macrocycle atoms of 0.15 Å, is less stable by ca. 4 kcal/mol. Additionally, structure i**P01** has a less conjugated thiazole−alkene system (C16−C17−C18−C19 torsional angles of −132.2° and −32.8° for i**P01** and i**X05**, respectively) and a slightly more tilted peptide bond (−24.0° and −20.1°, respectively). The repulsive interaction between the π-electrons of the alkene and the n-electrons of the lactone carbonyl may be partially responsible for this effect. Structure i**X12**, which also has the same hydrogen bond pattern as i**P01**, is ca. 8 kcal/mol less stable than the reference compound, even though, as above, the deconjugation of the thiazole−alkene system is less pronounced (C16−C17−C18−C19 torsional angles of 29.7° and −132.2° for i**X12** and i**P01**, respectively), and the distortion of the peptide bond from planarity is much smaller than in the reference structure (−18.0° and −24.0°, respectively). Note that i**X12** can cause local destabilization due to n−π repulsion

dx.doi.org/10.1021/jp212628v | J. Phys. Chem. B 2012, 116, 7605−7617

between the oxygen atom of the epoxide and the side chain double bond. Moreover, transannular hydrogen interactions (NH−H(C11) and H(C3)−H(C17)) have an appreciable impact on the overall conformational energy profile.

PCM Calculations. The solvation of epothilone involves screening by the surrounding dielectric medium, which should have significant effects on dipole−dipole interactions and hydrogen bonding. Therefore, the effect of solvent polarity on the stability of a given conformer could be associated with the intricate system of interactions between the polar functionalities. Considering that the featureless polarized continuum model with a standard dielectric constant of 4 is routinely employed to simulate the protein environment around the binding site,[60] this method appears to be effective for reproducing the shape and population of epothilone immediately before forming the ligand−protein complex.

The dielectric effects from the surroundings were obtained for protein environment, dichloromethane, dimethylsulfoxide, and water using the polarized continuum model.[50] Solvent effects were particularly pursued for the most stable representative conformations. Actually, general shapes, hydrogen bond lengths and hydrogen bond angles change only slightly over the entire range of dielectric constants. There were clear solvent effects on the energies of the patupilone conformers: the more polar the solvent (DCM < DMSO < water), the greater the decrease in the relative energy of reported structures b**M01** and b**M02** (by approximately 2.5 kcal/mol in water, compared to in a vacuum; Table SI4). The contribution percentages of these structures to the total population in water are 28.0% and 3.5%, respectively (11.2% and 8.8% for the protein dielectric constant). This result is not very surprising considering that an NMR experiment found a**M** to be the significant fraction in water[30] and the predominant conformer in water *in the presence* of tubulin.[29] More generally, my data reveal that in aqueous solution patupilone, as the *free* ligand, is represented exclusively as exo compact structures b**P**(48.5%), b**X**(20.1%), and the above-mentioned b**M**(31.5%; Table SI4). The torsional angles of b**P** and b**X** fit well to the ensemble of feasible torsions found for epothilone A (see Figure 2 in ref 30). Moreover, the score obtained for unbound epothilone A in aqueous solution with NAMFIS analysis[30] shows the participation of both syn- and antiperiplanar conformations for the C16−C17−C18−C19 to be 74% syn and 26% anti, in good agreement with ca. 80:20 ratio of our b**P** and b**M** (syn) and b**X** (anti) compact PCM conformers. Thus, it seems that b**P** and b**X** subsets equilibrate with b**M**, the experimental conformer known as an "NMR-derived tubulin-bound structure".[29]

The cyclic system of ixabepilone, which is stiffened by transannular hydrogen bonding, is evidently relatively resistant to conformational changes, but mutual interactions influence the final energy level. Conformers i**P**, i**T** and i**W**, which are important species at equilibrium in the vacuum, markedly increase in energy as the dielectric constant is increased. The opposite trend is observed for i**M** conformers. Their relative energies decrease from 4.59 and 7.13 kcal/mol (for i**M01** and i**M12**, respectively), to a global minimum level (the population of these two conformers in water is nearly 94%).

As discussed above, the data reported for patupilone show that in a protein environment, but particularly in water, the molecule is represented only by exo compact structures (b**M**, b**P**, and b**X** conformers). The exo crystal structure[2] b**H** and endo EC structure[18] b**S** were not found among the most stable conformers. The case of ixabepilone (Table SI9) is more complex because exo and endo conformers coexist within the protein space: i**X**, i**P** and i**M** conformers are supplemented with the i**W** subset. However, this is not the case in water, where exo species dominate. These results lead to the conclusion that the structural modifications to the macrocycle should have consequences on the ligand binding process.

CONCLUSIONS

As expected, there is a marked similarity between the geometries of patupilone (epothilone B) and epothilone A. The shapes of ixabepilone and patupilone are generally conserved if the pattern of hydrogen bonding is kept constant. All the stable conformers of patupilone are found to be exo and compact, commonly exhibiting 3-hydroxyl−thiazole and 7-hydroxyl−carbonyl hydrogen bonding motifs. The lactam structure of ixabepilone offers more hydrogen bonding patterns than the epothilone lactones. In contrast to patupilone, an ensemble of the most stable ixabepilone conformers includes two kinds of exo (including compact) conformations and one kind of endo conformation, which exploits the cooperative hydrogen bonding between the amide, the 3-hydroxyl, and the transannular epoxide. Calculations revealed that this point structural change in the macrocycle alters the conformational preferences of the macroring system. In all cases, the 3-hydroxyl group was found to play a key role in aligning hydrogen bonding within the molecule.[cf30]

PCM calculations indicated that, even though they have a hydrophobic shape,[42] the prediction of compact conformers is better in water than in the vacuum. The experimental b**M**[29] exo conformers, particularly the i**M** conformers, are highly sensitive to the polarity of the environment. The endo i**W** conformers, which compete favorably with the exo conformers for participation in the vacuum or in protein surroundings, are not at all represented in water. It is evident that the PES of ixabepilone is more diverse than that of patupilone, and these findings are in general agreement with the very recent report of deuterium incorporation into microtubules.[35] I hope that the considerable potential of solvent-dependent PES data for patupilone and ixabepilone may stimulate further efforts in the field. All aspects of the conformational analysis may be helpful for structural interpretations of the binding of epothilone to tubulin.

ASSOCIATED CONTENT

Supporting Information

Tables containing coordinates, energies of the optimized conformers of patupilone and ixabepilone, and other structural data. This material is available free of charge via the Internet at http://pubs.acs.org.

AUTHOR INFORMATION

Corresponding Author

*E-mail: Marek.Lozynski@put.poznan.pl; tel: (+48)61-665-3534; fax: (+48)61-665-3649.

Notes

The authors declare no competing financial interest.

ACKNOWLEDGMENTS

This study was supported by the Poznan University of Technology/DS 32/045/2011. I would also like to acknowl-

edge the Poznanskie Centrum Superkomputerowo−Sieciowe, Poznan, Poland for computational time.

REFERENCES

(1) Bollag, D. M.; McQueney, P. A.; Zhu, J.; Hensens, O.; Koupal, L.; Liesch, J.; Goetz, M.; Lazarides, E.; Woods, C. M. *Cancer Res.* **1995**, *55*, 2325−2333.

(2) Höfle, G.; Bedorf, N.; Steinmetz, H.; Schomburg, D.; Gerth, K.; Reichenbach, H. *Angew. Chem., Int. Ed. Engl.* **1996**, *35*, 1567−1569.

(3) Gerth, K.; Bedorf, N.; Höfle, G.; Irschik, H.; Reichenbach, H. *J. Antibiot.* **1996**, *49*, 560−563.

(4) Jordan, M. A. *Curr. Med. Chem.: Anti-Cancer Agents* **2002**, *2*, 1−17.

(5) Jordan, M. A.; Wilson, L. *Nat. Rev. Cancer* **2004**, *4*, 253−265.

(6) Lee, F. Y. F.; Borzilleri, R.; Fairchild, C. R.; Kim, S.-H.; Long, B. H.; Reventos-Suarez, C.; Vite, G. D.; Rose, W. C.; Kramer, R. A. *Clin. Cancer Res.* **2001**, *7*, 1429−1437.

(7) Cortes, J.; Baselga, J. *Oncologist* **2007**, *12*, 271−280.

(8) Borzilleri, R. M.; Zheng, X.; Schmidt, R. J.; Johnson, J. A.; Kim, S.-H.; DiMarco, J. D.; Fairchild, C. R.; Gougoutas, J. Z.; Lee, F. Y. F.; Long, B. H.; Vite, G. D. *J. Am. Chem. Soc.* **2000**, *122*, 8890−8897.

(9) Peterson, J. K.; Tucker, C.; Favours, E.; Cheshire, P. J.; Creech, J.; Billups, C. A.; Smykla, R.; Lee, F. Y. F.; Houghton, P. J. *Clin. Cancer Res.* **2005**, *11*, 6950−6958.

(10) Perez, E. A.; Lerzo, G.; Pivot, X.; Thomas, E.; Vahdat, L.; Bosserman, L.; Viens, P.; Cai, C.; Mullaney, B.; Peck, R.; Gabriel, N.; Hortobagyi, G. N. *J. Clin. Oncol.* **2007**, *25*, 3407−3414.

(11) Conlin, A.; Fornier, M.; Hudis, C.; Kar, S.; Kirkpatrick, P. *Nat. Rev. Drug Discovery* **2007**, *6*, 953−954.

(12) Gradishar, W. *Drug Des. Dev. Ther.* **2009**, *3*, 163−167.

(13) Gianni, L. *J. Clin. Oncol.* **2007**, *25*, 3389−3391.

(14) Diaz, J. F.; Menendez, M.; Andreu, J. M. *Biochemistry* **1993**, *32*, 10067−10077.

(15) Snyder, J. P.; Nettles, J. H.; Cornett, B.; Downing, K. H.; Nogales, E. *Proc. Natl. Acad. Sci. U.S.A.* **2001**, *98*, 5312−5316.

(16) Lowe, J.; Li, H.; Downing, K. H.; Nogales, E. *J. Mol. Biol.* **2001**, *313*, 1045−57.

(17) Makowski, L. *Nature* **1995**, *375*, 361−362.

(18) Nettles, J. H.; Li, H.; Cornett, B.; Krahn, J. M.; Snyder, J. P.; Downing, K. H. *Science* **2004**, *305*, 866−869.

(19) Winkler, J. D.; Axelsen, P. H. *Bioorg. Med. Chem. Lett.* **1996**, *6*, 2963−2966.

(20) Chakravarty, S.; Ojima, I. Presented at the 214th American Chemical Society Meeting, Las Vegas, NV; September 7−11, 1997 (MEDI 75).

(21) Giannakakou, P.; Gussio, R.; Nogales, E.; Downing, K. H.; Zaharevitz, D.; Bollbuck, B.; Poy, G.; Sackett, D.; Nicolaou, K. C.; Fojo, T. *Proc. Natl. Acad. Sci. U.S.A.* **2000**, *97*, 2904−2909.

(22) He, L.; Jagtap, P. G.; Kingston, D. G. I.; Shen, H.-J.; Orr, G. A.; Horwitz, S. B. *Bichemistry* **2000**, *39*, 3972−3978.

(23) Ojima, I.; Chakravarty, S.; Inoue, T.; Lin, S.; He, L.; Horwitz, S. B.; Kuduk, S. D.; Danishefsky, S. J. *Proc. Natl. Acad. Sci. U.S.A.* **1999**, *96*, 4256−4261.

(24) Sanchez-Pedegral, V. M.; Kubicek, K.; Meiler, J.; Lyothier, I.; Paterson, I.; Carlomagno, T. *Angew. Chem., Int. Ed.* **2006**, *45*, 7388−7394.

(25) Reese, M.; Sánchez-Pedregal, V. M.; Kubicek, K.; Meiler, J; Blommers, M. J. J.; Griesinger, C.; Carlomagno, T. *Angew. Chem., Int. Ed.* **2007**, *46*, 1864−1868.

(26) Heinz, D. W.; Schubert, W.-D.; Höfle, G. *Angew. Chem., Int. Ed.* **2005**, *44*, 1298−1301.

(27) Nettles, J. H.; Downing, K. H. The Tubulin Binding Mode of Microtubule Stabilizing Agents Studied by Electron Crystallography. In *Tubulin-Binding Agents: Synthetic, Structural and Mechanistic Insights*; Carlomagno, T., Ed.; Springer-Verlag: Berlin Heidelberg, 2009; Vol. *286*, pp 209−257.

(28) Stanton, R. A.; Gernert, K. M.; Nettles, J. H.; Aneja, R. *Med. Res. Rev.* **2011**, *31*, 443−481.

(29) Carlomagno, T.; Blommers, M. J. J.; Meiler, J.; Jahnke, W.; Schupp, T.; Petersen, F.; Schinzer, D.; Altmann, K.-H.; Griesinger, C. *Angew. Chem., Int. Ed.* **2003**, *42*, 2511−2515.

(30) Erdélyi, M.; Pfeiffer, B.; Hauenstein, K.; Fohrer, J.; Gertsch, J.; Altmann, K.-H.; Carlomagno, T. *J. Med. Chem.* **2008**, *51*, 1469−1473.

(31) Lange, A.; Schupp, T.; Petersen, F.; Carlomagno, T.; Baldus, M. *ChemMedChem* **2007**, *2*, 522−527.

(32) Kumar, A.; Heise, H.; Blommers, M. J. J.; Krastel, P.; Schmitt, E.; Petersen, F.; Jeganathan, S.; Mandelkow, E.-M.; Carlomagno, T.; Griesinger, C.; Baldus, M. *Angew. Chem., Int. Ed.* **2010**, *49*, 7504−7507.

(33) Xiao, H.; Verdier-Pinard, P.; Fernandez-Fuentes, N.; Burd, B.; Angeletti, R.; Fiser, A.; Horwitz, S. B.; Orr, G. A. *Proc. Natl. Acad. Sci. U.S.A.* **2006**, *103*, 10166−10173.

(34) Khrapunovich-Baine, M.; Menon, V.; Verdier-Pinard, P.; Smith, A. B., III; Angeletti, R. H.; Fiser, A.; Horwitz, S. B.; Xiao, H. *Biochemistry* **2009**, *48*, 11664−11677.

(35) Khrapunovich-Baine, M.; Menon, V.; Yang, Ch.-P. H.; Northcote, P.; Miller, J. H.; Angeletti, R. H.; Fiser, A.; Horwitz, S. B.; Xiao, H. *J. Biol. Chem.* **2011**, *286*, 11765−11778.

(36) Dumontet, Ch.; Jordan, M. A. *Nat. Rev. Drug Discovery* **2010**, *9*, 790−803.

(37) Krause, W.; Klar, U. *Curr. Cancer Ther. Rev.* **2011**, *7*, 10−36.

(38) Dumontet, Ch.; Jordan, M. A.; Lee, F. Y. F. *Mol. Cancer Ther.* **2009**, *8*, 17−25.

(39) Kamel, K.; Rusinska-Roszak, D. *Int. J. Quantum Chem.* **2008**, *108*, 967−973.

(40) Rusinska-Roszak, D.; Lozynski, M. *J. Mol. Model.* **2009**, *15*, 859−869.

(41) Jimenez, V. A. *J. Chem. Inf. Model.* **2010**, *50*, 2176−2190.

(42) Rusinska-Roszak, D.; Tatka, H.; Pawlak, R.; Lozynski, M. *J. Phys. Chem. B* **2011**, *115*, 3698−3707.

(43) Nagano, S.; Li, H.; Shimizu, H.; Nishida, C.; Ogura, H.; de Montellano, P. R. O.; Poulos, T. L. *J. Biol. Chem.* **2003**, *278*, 44886−44893.

(44) Taylor, R. E.; Zajicek, J. *J. Org. Chem.* **1999**, *64*, 7224−7228.

(45) Wang, M.; Xia, X.; Kim, Y.; Hwang, D.; Jansen, J. M.; Botta, M.; Liotta, D. C.; Snyder, J. P. *Org. Lett.* **1999**, *1*, 43−46.

(46) RCSB Protein Data Bank. http://www.pdb.org.

(47) Jones, G. A.; Paddon-Row, M. N.; Sherburn, M. S.; Turner, C. I. *Org. Lett.* **2002**, *4*, 3789−3792.

(48) Bakalova, S. M.; Gil Santos, A. G. *J. Org. Chem.* **2004**, *69*, 8475−8481.

(49) Frisch, M. J. et al. *Gaussian 09*, revision B.01; Gaussian, Inc.: Wallingford, CT, 2010.

(50) Scalmani, G.; Frisch, M. J. *J. Chem. Phys.* **2010**, *132*, 114110.

(51) Mulzer, J.; Altmann, K.-H.; Höfle, G.; Müller, R.; Prantz, K. *C. R. Chim.* **2008**, *11*, 1336−1368.

(52) Nicolaou, K. C.; Ritzén, A.; Namoto, K. *Chem. Commun.* **2001**, 1523−1535.

(53) Nicolaou, K. C.; Vourloumis, D.; Li, T.; Pastor, J.; Winssinger, N.; He, Y.; Ninkovic, S.; Sarabia, F.; Vallberg, H.; Roschangar, F.; King, N. P.; Finlay, M. R. V.; Giannakakou, P.; Verdier-Pinard, P.; Hamel, E. *Angew. Chem., Int. Ed. Engl.* **1997**, *36*, 2097−2103.

(54) Nicolaou, K. C.; Scarpelli, R.; Bollbuck, B.; Werschkun, B.; Pereira, M. M. A.; Wartmann, M.; Altmann, K.-H.; Zaharewitz, D.; Gussio, R.; Giannakakou, P. *Chem. Biol.* **2000**, *7*, 593−599.

(55) Nicolaou, K. C.; Pratt, B. A.; Arseniyadis, S.; Wartmann, M.; O'Brate, A.; Giannakakou, P. *ChemMedChem* **2006**, *1*, 41−44.

(56) Altmann, K.-H.; Bold, G.; Caravatti, G.; Florsheimer, A.; Guagnano, V.; Wartmann, M. *Bioorg. Med. Chem. Lett.* **2000**, *10*, 2765−2768.

(57) Altmann, K.-H.; Bold, G.; Caravatti, G.; End, N.; Florsheimer, A.; Guagnano, V.; O'Reilly, T.; Wartmann, M. *Chimia* **2000**, *54*, 612−621.

(58) Bondi, A. *J. Phys. Chem.* **1964**, *68*, 441−451.

(59) Jeffrey, G. A.; Saenger, W. *Hydrogen Bonding in Biological Structures*; Springer Verlag: Berlin, 1994; Chapter 2.

(60) Harvey, S. C. *Proteins* **1989**, *5*, 78−92.